



**HAL**  
open science

# Microstructural Characterization of Oolitic Rocks and Numerical Evaluation of their Effective Elastic Properties

Kassem Kalo, Dragan Grgic, Christophe Auvray, Albert Giraud

► **To cite this version:**

Kassem Kalo, Dragan Grgic, Christophe Auvray, Albert Giraud. Microstructural Characterization of Oolitic Rocks and Numerical Evaluation of their Effective Elastic Properties. *Procedia Engineering*, 2017, 191, pp.59-66. 10.1016/j.proeng.2017.05.154 . hal-02981397

**HAL Id: hal-02981397**

**<https://hal.univ-lorraine.fr/hal-02981397>**

Submitted on 28 Oct 2020

**HAL** is a multi-disciplinary open access archive for the deposit and dissemination of scientific research documents, whether they are published or not. The documents may come from teaching and research institutions in France or abroad, or from public or private research centers.

L'archive ouverte pluridisciplinaire **HAL**, est destinée au dépôt et à la diffusion de documents scientifiques de niveau recherche, publiés ou non, émanant des établissements d'enseignement et de recherche français ou étrangers, des laboratoires publics ou privés.



Distributed under a Creative Commons Attribution - NoDerivatives 4.0 International License



Symposium of the International Society for Rock Mechanics

## Microstructural Characterization of Oolitic Rocks and Numerical Evaluation of Their Effective Elastic Properties

Kassem Kalo, Dragan Grgic\*, Christophe Auvray, Albert Giraud

*GeoResources Laboratory, Université de Lorraine (ENSG), CNRS, CREGU, F-54501, Vandoeuvre-les-Nancy, France*

---

### Abstract

The present work focuses on the characterization of the geometry of the microstructure of porous oolitic rocks. These rocks are constituted by an assemblage of porous grains (oolites), pores and inter-granular crystals. X ray 3D Computed Tomography is used to identify the different components of these rocks by applying an algorithm based on grayscale values. This analytical method allows the characterization of the porous network (size, spatial distribution, and volume fraction), oolites and inter-oolitic crystals. The microstructure of these porous rocks has a significant effect on their macroscopic behavior. This micro-macroscopic relationship is taken into account in micromechanical models developed within the framework of the homogenization theory (e.g., Maxwell scheme) of random heterogeneous media. X ray tomography images showed that pores have irregular shapes, so the micromechanical modeling based on analytical solution is not relevant. Then, pores are approximated by ellipsoids using principal components analysis (PCA) method, which allows us to obtain the geometrical properties such as length of semi-axes and orientation of ellipsoids. To validate mechanically this approximation, we compared the contribution of irregularly shaped 3D pores and ellipsoidal pores to the effective elastic properties. The relative error due to this ellipsoidal approximation is then estimated. The compliance contribution tensors of irregular 3D pores are evaluated numerically using finite element method while those of approximated ellipsoidal pores are obtained analytically and numerically. The same procedure of approximation is applied on oolites. Shape and spatial parameters, such as the volume, radius and center of each oolite are also determined. The sphericity of the approximated oolites is calculated. The obtained values are close to 1, so oolites can be reasonably approximated by spheres.

© 2017 Published by Elsevier Ltd. This is an open access article under the CC BY-NC-ND license

(<http://creativecommons.org/licenses/by-nc-nd/4.0/>).

Peer-review under responsibility of the organizing committee of EUROCK 2017

*Keywords:* Compliance contribution tensor; Microstructural analysis; Finite element method; 3D irregular shape inhomogeneities

---

---

\* Corresponding author. Tel.: +33-3-83596369.

E-mail address: [dragan.grgic@univ-lorraine.fr](mailto:dragan.grgic@univ-lorraine.fr)

## 1. Introduction

In this paper, we characterize the geometry of porous oolitic rocks that are modeled as a heterogeneous material composed by an assemblage of porous grains (oolites), pores and inter-granular crystals (cement). We used a simplified model within the framework of Maxwell homogenization scheme described in [1]. Three scales are then identified. First is the microscopic scale that corresponds to the intra-oolitic pores. Second is the mesoscopic scale that corresponds to the oolites, the inter-oolitic cement and pores. Third is the largest scale and corresponds to the representative elementary volume (REV) which is considered large compared to the oolites size, the intra and inter-oolitic pores. The first homogenization step concerns intra-oolitic pores of spherical or ellipsoidal shape within oolites using Self Consistent Approximation [2]. It allows the transition from the microscopic to the mesoscopic scale. The second step allows the transition from the mesoscopic to the macroscopic scale using Maxwell homogenization scheme. As in [1], at the mesoscopic scale we consider that the heterogeneous medium is formed by three phases: the porous oolites approximated by spheres, inter-oolitic cement and irregularly shaped pores approximated by ellipsoids with randomly distributed orientation. This Maxwell model and its reformulation based on contribution tensors are discussed in [3, 4, 5, 6]. Indeed, this method has been used by [7] for the calculation of effective parameters of poroelastic composite materials. This method has also been extended in [8] to the case of viscoelastic microcracked materials. In our study, we considered an oolitic limestone as heterogeneous material. To verify the homogenization method, we approximate the rock components by the PCA method presented in [9] as follows: oolites are approximated by spheres and interoolitic pores are approximated by ellipsoids. The microstructure of the material was observed using 3D X-ray nano-computed tomography and scanning electron microscopy. We analyze then the X-Ray images using image processing software in order to distinguish the different components of the material. The procedure for the geometry analysis of oolites and pores is presented in section 2. To validate the approximation, we evaluate the contribution of irregularly shaped 3D pores and ellipsoidal pores to the effective elastic properties. Our work is based on the previous calculation of compliance contribution tensors of 3D pores of irregular shape in carbon/carbon composites [9]. Analytical method based on Eshelby solution for ellipsoidal shapes are usually used to evaluate the contribution of pores to effective elastic properties. However, in our case, this solution is not relevant due to the high irregularity of the pores, so numerical methods such as finite element method (FEA) is used. The FEA procedure for the evaluation of the contribution tensors of irregular shape pores and their corresponding ellipsoids is presented in section 3. Then, we evaluated analytically the contribution tensors of the ellipsoids and we estimate the relative error due to this approximation.

## 2. Microscopic observations of a porous oolitic limestone (Lavoux, France)

### 2.1. SEM observation

Lavoux limestone is a middle Jurassic (Callovian) oolitic limestone, located in the southwest of the Paris Basin, in Vienne, France [10]. To observe the microstructure of the rock, two techniques were used: SEM (scanning electron microscope) (Fig. 1) and 3D X-ray nanotomography. The microstructure of oolitic limestone observed under SEM is described in [11].

Chemical characterization performed on the limestone Lavoux by the EDS method (Energy Dispersive X-ray Spectroscopy) showed that the material is mainly composed of calcite (98%) and contains also a very small fraction of clays and dolomite [11]. So it is almost a mono-mineral limestone.

Within the homogenization framework, this description allows us to consider the microstructure of the limestone as an assembly of grains (oolites) and inter-oolitic pores. Indeed, there are two scales in the microstructure of the material:

- The mesoscopic scale (sample level) is primarily that of oolites and inter-oolitic meso and macro pores.
- The microscopic scale is that of the micro-pores in oolites.

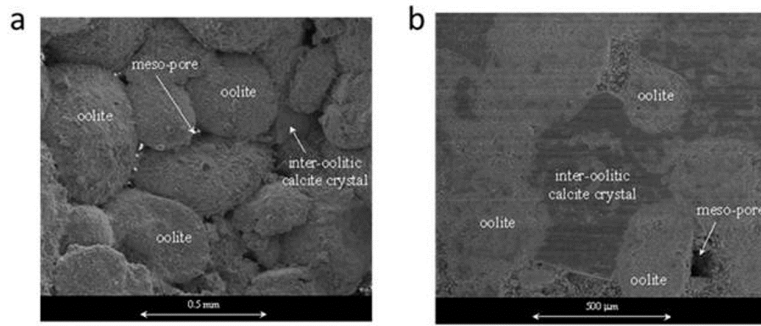


Fig. 1. SEM (scanning electron microscope) images of Lavoux limestone.

## 2.2. 3D X-Ray computed tomography

The scan of a limestone sample (diameter = 5 mm, resolution (voxel size) = 5  $\mu\text{m}$ ) was performed using a 3D X-ray nanotomograph. Tomographic images are reconstructed and a thresholding algorithm is applied to characterize the microstructure. To obtain the pore structure for future micromechanical modelling, a representative elementary volume (REV) is selected from the binary database. REV is defined as the smallest volume where the measurements of the physical properties are representative of the entire volume [12]. The analysis of the REV using image processing software showed that the limestone consists of three main components (Fig. 2): oolites having more or less spherical shape, interoolitic pores having irregular shapes, and interoolitic crystals (cement).

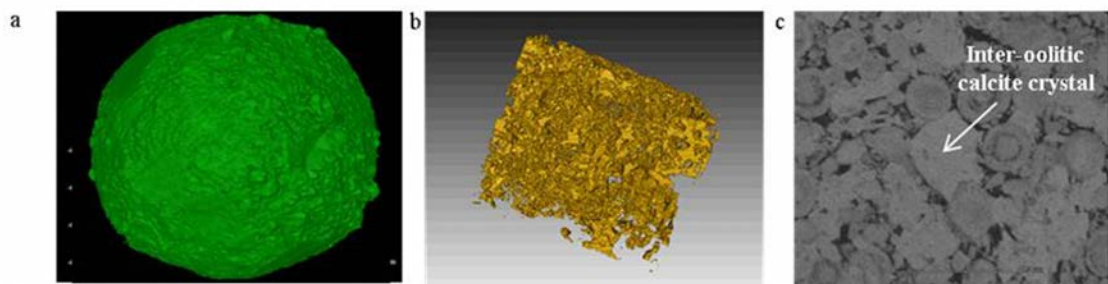


Fig. 2. Main components of the limestone in the REV using X-ray 3D nanotomography: (a) oolite; (b) porous network; (c) interoolitic crystal.

Using the database of the REV and a segmentation algorithm based on the grayscale values, we obtained the porous network of the REV (Fig. 2). The calculated porosity is equal to 6.9% and it represents the volume of inter-oolitic pores (meso and macro pores) over the total volume. Micropores inside oolites are not taken into account because they are not accessible due to the limitation of the resolution (5 micrometers) of X-ray tomography images. We compare this porosity value with the porosity obtained with the mercury porosimetry method described in [13] which allows to access very small pore radius. By considering pore radius larger than 5 micrometers, which corresponds to the tomography resolution, mercury porosity is equal to 7%, which is very close to 6.9%.

## 3. Approximation of irregularly shaped elements by ellipsoids

### 3.1. Pores

The approximation of irregularly shaped pores by ellipsoids can be based on several parameters depending on the application domain. In fact, two issues may arise: the first is the choice of the best approximation of pores shape

by ellipsoid (orientations and lengths of the principal axes) and the second is the accuracy of the selected approximation [9]. In this paper, we focus on mechanical applications that require the conservation of moments of inertia of initial pores shape. Indeed, we chose the PCA method. This method based on moments of inertia gives us the length and the orientation of the three principal axes of the ellipsoid. The following procedure was used:

- 3D acquisition of real pore (Fig. 3. (a,b))
- Pore mesh and extracting of surface points (Fig. 3 (c))
- Ellipsoidal approximation based on the PCA method

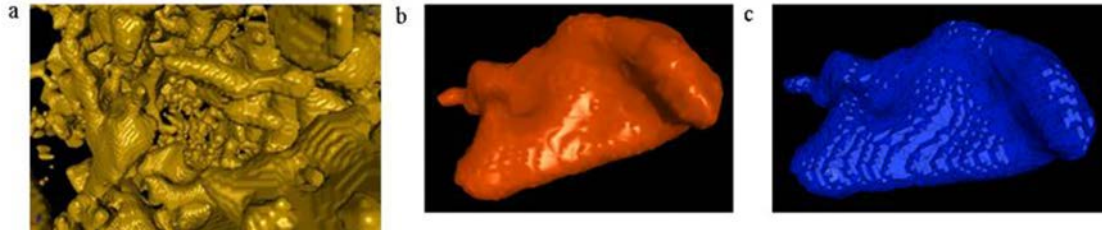


Fig. 3. (a) 3D view of porous network; (b) 3D view of a selected pore; (c) surface mesh.

The definition of the covariance matrix of the surface points is as follows:

$$C = \begin{pmatrix} \text{cov}(x,x) & \text{cov}(x,y) & \text{cov}(x,z) \\ \text{cov}(y,x) & \text{cov}(y,y) & \text{cov}(y,z) \\ \text{cov}(z,x) & \text{cov}(z,y) & \text{cov}(z,z) \end{pmatrix} \quad (1)$$

This matrix is symmetric. By applying normal vectors decomposition, we rewrite this matrix as a function of eigenvectors and eigenvalues [14] as follows:

$$C = Q\Lambda Q^T \quad (2)$$

Where  $Q$  is the matrix of eigenvectors representing the direction of the 3 axes of the ellipsoid and  $\Lambda$  is the eigenvalues matrix having  $\lambda_i$   $i = 1, 2, 3$  as diagonal terms where  $2\sqrt{\lambda_i}$  are the lengths of the three major semi-axes  $a, b$  and  $c$  of the ellipsoid. The results obtained for one pore of the selected REV are shown in Fig. 4:  $a = 0.16$  mm,  $b = 0.0704$  mm and  $c = 0.0465$  mm.

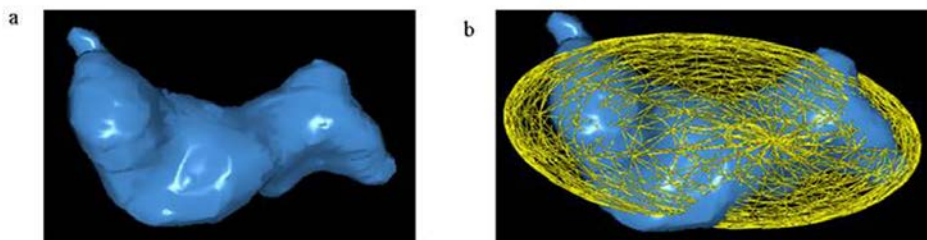


Fig. 4. (a) 3D view of a selected pore; (b) approximation of the pore by ellipsoid using the PCA method.

### 3.2. Oolites

In this section, we study the geometry of the oolites which are approximated by spheres in the simplified Maxwell model [1]. To verify this approximation, we calculate the sphericity ratio of oolites. In literature, sphericity is defined as the ratio between the surface of the oolite if considered as a sphere and its real surface. Many parameters related to the geometry can affect the estimation of the sphericity such as the surface area. If this area is not properly taken into account, the obtained values of sphericity may be affected. We extracted oolites from X-Ray tomography images by image processing software based on grayscale values (material density). However, the Lavoux limestone is a mono-mineral (calcite) material, which makes the identification of the true edges of oolites surface a difficult process. To solve this problem, the following modified procedure was used:

- The limestone Lavoux sample is grinded to separate the oolites from other components.
- The oolites are extracted manually under a binocular microscope.
- The 50 selected oolites are put into a gel and a nanotomography scan is performed for the total sample (gel + oolites).
- Oolites are then approximated by ellipsoids using the PCA method (Fig. 5) to obtain a smooth surface area. Fig. 6. b. shows different calculated values of sphericity ratio. These values are close to 1, and then oolites can be reasonably approximated by spheres.

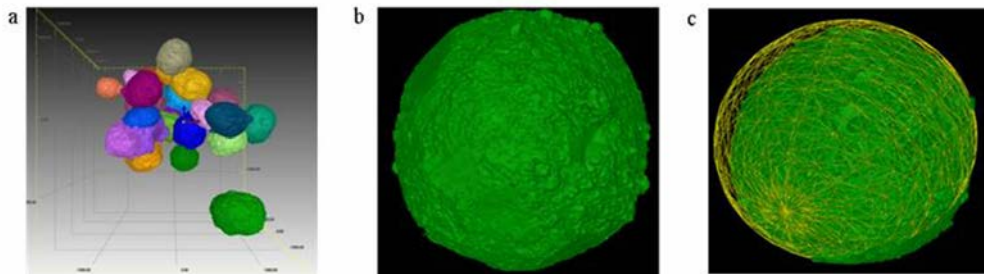


Fig. 5. (a) 3D view of some selected oolites in the VER; (b) 3D view of a selected oolite; (c) Approximation of the oolite by ellipsoid using PCA.

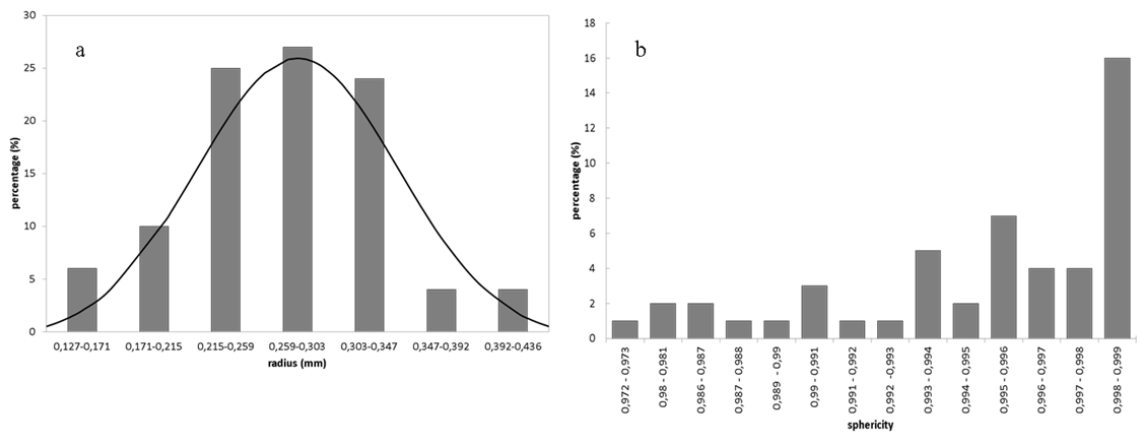


Fig. 6. Sphericity values for approximated oolites.

Fig. 6. shows that the radius of the oolites follows a normal distribution. In other words, the radius values of the oolites are between 0.127mm and 0.416 mm with a concentration in the center average.

#### 4. Property contribution tensors of a 3D irregularly shaped pore

To validate mechanically the approximation of pores by ellipsoids, we compare the contribution tensors (compliance) of pores to effective elastic properties with those of ellipsoids. Indeed, the presence of the pore in a material subjected to a uniform stress generates an additional strain. These tensors aim essentially to estimate the effective elastic properties of heterogeneous materials. Compliance tensors have been first introduced in the context of pores and cracks by [15]. 2D pores of different shapes and 3D pores of ellipsoidal shape have been studied by [16] and compliance tensors for these pores have been calculated. Many analytical and numerical results were obtained for 2D non-ellipsoidal pores by [17,18] which is not the case in our study. Indeed, microscopic observations on Lavoux limestone showed that pores have three dimensional irregular shapes. [9] calculated the contribution tensor for 3D pores of irregular shapes in carbon /carbon composite. Elastic and conductive properties of materials containing concave pores have been evaluated by [19]. In this section, we will evaluate numerically the elastic (compliance) contribution tensor of irregular pores in the Lavoux limestone and their corresponding ellipsoids using the finite element method. Then, the results for the ellipsoids are validated analytically and an error between the real pores tensor and their approximations is finally estimated. We consider the REV as a homogeneous elastic matrix of volume  $V$  containing an inhomogeneity of volume  $V^*$ . The compliance contribution tensor of this inhomogeneity is a fourth-rank tensor  $H$ . Its determination in the framework of Maxwell homogenization theory needs the calculation of the volume average of strain tensor in the inclusion.

$$\Delta \varepsilon = \frac{V}{V^*} H : \sigma^\infty \quad (3)$$

Where  $\sigma^\infty$  represents the applied stresses at the infinity, which is assumed to be uniform in the absence of the inhomogeneity. Furthermore, introducing  $\underline{n}$  as the outward unit vector to the boundary  $\partial\Omega$  of the inclusion and using the gradient formula of Gauss theorem, volume integral of strain tensor may be replaced by a surface integral [20]. This extra strain is given by [3] as an integral over the boundary of the pore  $\delta\Omega$  as follows:

$$\Delta \varepsilon_{ij} = \frac{-1}{2V} \int_{\partial\Omega} (u_i n_j + u_j n_i) dS \quad (4)$$

Where  $u$  and  $n$  are respectively the displacements at the boundary of the pore and  $n$  the normal vector.

Compliance contribution tensor is characterized by 21 independent components. To evaluate the integral (4), 3D finite element simulation was performed with Code\_Aster (EDF) using the following procedure:

- One extracted pore (volume = 0.001375 mm<sup>3</sup>) from nanotomography images is approximated by PCA method. The resulting ellipsoid has the following semi-axes lengths:  $a = 0.16$  mm,  $b = 0.0704$  mm and  $c = 0.0465$  mm. The volume of the approximated ellipsoid is:

$$V^* = \frac{4}{3} \pi abc = 0.0023 \text{ mm}^3 \quad (5)$$

- The pore and its approximated ellipsoid are placed separately into a cube with limits five times larger than the largest dimension of the pore. These models (cube + pore and cube + ellipsoid) were meshed using quadratic isoparametric Lagrange finite elements: 10-nodes tetrahedrons have been used for volume discretization and 6-nodes triangles have been used to discretize the surface of the pore and the ellipsoid.
- Boundary conditions were applied in terms of displacements. In order to obtain all 21 components, six load cases were considered as follow: 3 uniaxial tension in respectively  $x$ ,  $y$ ,  $z$  direction and 3 shear deformation in  $xy$ ,  $xz$ ,  $yz$  planes.

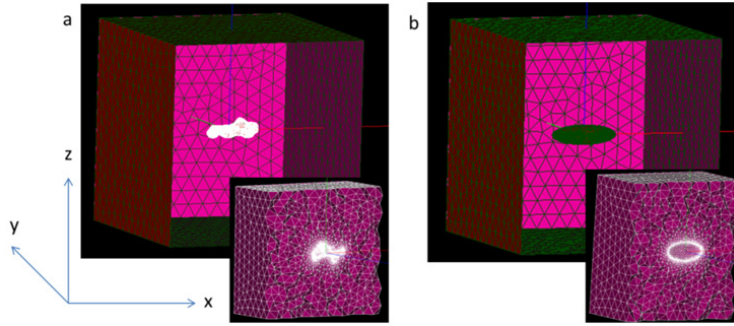


Fig. 7. Mesh of: (a) pore placed into a cube; (b) ellipsoid placed into a cube.

The normal vector to the surface is calculated at Gauss points using both analytical (for ellipsoid) and numerical (for pore and ellipsoid) solutions and then H tensor is evaluated using relation (3). The analytical solution is described in [22]. The normal vector is calculated numerically using nodes coordinates (as the cross product of 2 edges of surface) and interpolation formulas of Gauss Legendre [21]. The non-zero components of resulting H tensor for the selected ellipsoid using numerical and analytical solutions are given in table 1.

Table 1. Comparison between analytical and numerical H-tensor for one ellipsoid.

H tensor components	$H_{1111}$	$H_{1122}$	$H_{1133}$	$H_{2222}$	$H_{2233}$	$H_{3333}$	$H_{1212}$	$H_{2323}$	$H_{1313}$
Analytical results	1.268	0.2936	0.9308	2.0109	0.7448	3.7036	0.7739	1.64079	1.4183
Numerical results	1.259	0.2922	0.9318	2.0988	0.7456	3.7066	0.7753	1.6415	1.42303
Relative error (%)	0.7097	0.4768	0.1074	4.1881	0.1074	0.081	0.1809	0.0432	0.3335

The same procedure was applied on the selected pore and the H tensor is evaluated numerically. All components of the H-tensor for the pore shape shown in Fig. 4. can be evaluated and presented in the matrix form (Walpole convention) as follows:

Table 2. Numerical results for H-tensor components.

H tensor components	$H_{1111}$	$H_{1122}$	$H_{1133}$	$H_{2222}$	$H_{2233}$	$H_{3333}$	$H_{1212}$	$H_{2323}$	$H_{1313}$
Numerical results	1.863	0.199	0.758	2.160	0.314	4.255	1.11	2.143	1.844

Comparing the components of the 2 matrices, we observe that diagonal components are relatively close. No conclusions can be made for non-diagonal components. So to determine the efficiency of the approximation, we evaluated the distance  $\Delta$  between the H-tensors of the pore and the ellipsoid. We used the Euclidean norm for a fourth rank tensor given by:

$$\|S\| = \sqrt{S_{ijkl} S_{ijkl}} \tag{6}$$

$$\Delta = \frac{\|S^{pore} - S^{ellipsoide}\|}{\|S^{pore}\|} = 0.18 \tag{7}$$

This distance shows a difference of 18% between the compliance contribution tensor of the real pore and its approximation. Hence, we can reasonably consider that the approximation of a pore by an ellipsoid is relevant from a mechanical point of view. Further calculations on other pores are in progress.

## 5. Conclusion

We studied the geometry of the microstructure of a heterogeneous rock (oolitic limestone from Lavoux). The microstructure of this rock was observed under SEM and X-ray nanotomograph. These microstructural observations showed that the limestone Lavoux is formed by three main components: oolites, inter-oolitic pores and calcite crystals. In order to apply the homogenization method of Maxwell, a simplified model was considered: oolites are approximated by spheres and pores are approximated by ellipsoids. PCA approximation method is used for these approximations. It gives the 3 axes of inertia of the corresponding ellipsoid. The sphericity of the oolites approximated by ellipsoids is very close to 1 so they can be considered as spheres. To validate mechanically the approximation of pores by ellipsoids, contribution tensor (compliance) of pores and ellipsoids to effective elastic properties are evaluated. The compliance tensor for the ellipsoid is calculated numerically and analytically. The results showed that these 2 tensors are very close. The compliance tensor for real pores is evaluated numerically using interpolation formula of Gauss Legendre. The relative distance between this compliance contribution tensor and that of the ellipsoid is equal to 18%. Hence, from these first results, the approximation of a pore by an ellipsoid seems to be relevant from a mechanical point of view.

## References

- [1] A. Giraud, I. Sevostianov, F. Chen, D. Grgic, Effective thermal conductivity of oolitic rocks using the Maxwell homogenization method, *International Journal of Rock Mechanics & Mining Sciences* 80 (2015) 379–387.
- [2] D. Bruggeman, Berechnung verschiedener Physicalischer Konstanten von heterogenen Substanzen, I. Dielektrizitätskonstanten und Leitfähigkeiten der Mischkörper aus isotropen Substanzen, *Ann Physik* 416(7) (1935) 636–664.
- [3] I. Sevostianov, A. Giraud, Generalization of Maxwell homogenization scheme for elastic material containing inhomogeneities of diverse shape, *Int J Eng Sci.* 64 (2013) 23–36.
- [4] I. Sevostianov, On the shape of effective inclusion in the Maxwell homogenization scheme for anisotropic elastic composites, *Mech. Materials* 75 (2014) 45–59.
- [5] A. Giraud, I. Sevostianov, Micromechanical modeling of the effective elastic properties of oolitic limestone, *Int. J. Rock Mech. Min. Sci.* 62 (2013) 23–27.
- [6] V. I. Kushch, I. Sevostianov, Dipole moments, property contribution tensors and effective conductivity of anisotropic particulate composites, *International Journal of Engineering Science* 74 (2014) 15–34.
- [7] V. Levin, S. Kanaun, M. Markov, Generalized Maxwell's scheme for homogenization of poroelastic composites, *Int J Eng Sci.* 61(1) (2012) 75–86.
- [8] I. Sevostianov, V. Levin, E. Radi, Effective properties of linear viscoelastic microcracked materials: application of Maxwell homogenization scheme, *Mech Mater* 84 (2015) 28–43.
- [9] B. Drach, I. Tsukrov, T. Gross, S. Dietrich, K. Weidenmann, R. Piat, T. Bohlke, Numerical modeling of carbon/carbon composites with nanotextured matrix and 3D pores of irregular shape, *Int. J. Sol. Struct.* 48 (2011) 2447–2457.
- [10] J. Sterpenich, J. Sausse, J. Pironon, A. Gehin, G. Hubert, E. Perfetti, D. Grgic, Experimental ageing of oolitic limestones under CO<sub>2</sub> storage conditions. Petrographical and chemical evidence, *Chem Geol.* 265(1–2) (2009) 99–112.
- [11] N.B. Nguyen, A. Giraud, D. Grgic, A composite sphere assemblage model for oolitic rocks, *Int J Rock Mech Min Sci.* 48 (2011) 909–921.
- [12] S. Rolland du Roscoat, M. Decain, X. Thibault, C. Geindreau, J.-F. Bloch, Estimation of microstructural properties from synchrotron X-ray microtomography and determination of the REV in paper materials, *Acta Materialia* 55 (2007) 2841–2850.
- [13] D. Grgic, The influence of CO<sub>2</sub> on the long-term chemo-mechanical behavior of an oolitic limestone, *J. Geophys. Res.* 116(B7) (2011) 2156–2202.
- [14] I.N. Bronstein, K.A. Semendjajew, *Taschenbuch der Mathematik*. Auflage, BG Teubner Verlagsgesellschaft, Stuttgart Leipzig und Verlag Nauka, Moskau, 2006.
- [15] H. Horii, S. Nemat-Nasser, Overall moduli of solids with microcracks: load-induced anisotropy, *J. Mech. Phys. Solids* 31(1983) 155–171.
- [16] M. Kachanov, I. Tsukrov, B. Shafiro, Effective moduli of solids with cavities of various shapes, *Appl. Mech. Rev.* 47 (1994) S151–S174.
- [17] I. Tsukrov, J. Novak, Effective elastic properties of solids with defects of irregular shape, *Int. J. Solids Struct.* 39 (2002) 1539–1555.
- [18] R.W. Zimmerman, Compressibility of two-dimensional cavities of various shapes, *J. Appl. Mech.* 53 (1986) 500–504.
- [19] F. Chen, I. Sevostianov, A. Giraud, D. Grgic, Evaluation of the effective elastic and conductive properties of a material containing concave pores, *International Journal of Engineering Science* 97 (2015) 60–68.
- [20] I. Sevostianov, A. Giraud, Generalization of Maxwell homogenization scheme for elastic material containing inhomogeneities of diverse shape, *International Journal of Engineering Science* 64 (0) (2013) 23 – 36.
- [21] I. Sevostianov, F. Chen, A. Giraud, D. Grgic, Compliance and resistivity contribution tensors of axisymmetric concave pores, *International Journal of Engineering Science* 101 (2016) 14–28.